AFRL-RZ-WP-TP-2010-2025

CURRENT SCALING IN AN ATMOSPHERIC PRESSURE CAPILLARY DIELECTRIC BARRIER DISCHARGE (POSTPRINT)

Biswa N. Ganguly

Energy and Power Systems Branch
Energy/Power/Thermal Division

Brian L. Sands

UES, Inc.

Shih K. Huang

Wright State University

JANUARY 2010

AIR FORCE RESEARCH LABORATORY
PROPULSION DIRECTORATE
WRIGHT-PATTERSON AIR FORCE BASE, OH 45433-7251
AIR FORCE MATERIEL COMMAND
UNITED STATES AIR FORCE

REPORT DOCUMENTATION PAGE

Form Approved
OMB No. 0704-0188

1. REPORT DATE *(DD-MM-YY)*	2. REPORT TYPE	3. DATES COVERED *(From - To)*
January 2010	Journal Article Postprint	01 October 2007 – 31 December 2009

4. TITLE AND SUBTITLE
CURRENT SCALING IN AN ATMOSPHERIC PRESSURE CAPILLARY DIELECTRIC BARRIER DISCHARGE (POSTPRINT)

5a. CONTRACT NUMBER
In-house

5b. GRANT NUMBER

5c. PROGRAM ELEMENT NUMBER
61102F

6. AUTHOR(S)
Biswa N. Ganguly (AFRL/RZPE)
Brian L. Sands (UES, Inc.)
Shih K. Huang (Wright State University)

5d. PROJECT NUMBER
2301

5e. TASK NUMBER
29

5f. WORK UNIT NUMBER
23012900

7. PERFORMING ORGANIZATION NAME(S) AND ADDRESS(ES)
Energy and Power Systems Branch (AFRL/RZPE)
Energy/Power/Thermal Division
Air Force Research Laboratory, Propulsion Directorate
Wright-Patterson Air Force Base, OH 45433-7251
Air Force Materiel Command, United States Air Force

UES, Inc.
4401 Dayton-Xenia Road
Dayton, OH 45432

Wright State University
Department of Mechanical and Materials Engineering
3640 Colonel Glenn Highway
Dayton, OH 45435

8. PERFORMING ORGANIZATION REPORT NUMBER
AFRL-RZ-WP-TP-2010-2025

9. SPONSORING/MONITORING AGENCY NAME(S) AND ADDRESS(ES)
Air Force Research Laboratory
Propulsion Directorate
Wright-Patterson Air Force Base, OH 45433-7251
Air Force Materiel Command
United States Air Force

10. SPONSORING/MONITORING AGENCY ACRONYM(S)
AFRL/RZPE

11. SPONSORING/MONITORING AGENCY REPORT NUMBER(S)
AFRL-RZ-WP-TP-2010-2025

12. DISTRIBUTION/AVAILABILITY STATEMENT
Approved for public release; distribution unlimited.

13. SUPPLEMENTARY NOTES
Journal article published in *Applied Physics Letters*, Vol. 95, 051502 (2009). PA Case Number: 88ABW-2009-3421; Clearance Date: 24 Jul 2009. Paper contains color.

14. ABSTRACT
Current scaling in an atmospheric pressure capillary dielectric barrier discharge, comprising a structured rare gas flow that extends into ambient air, is characterized by electrical and optical measurements. In the transient glow mode, two current scaling regimes were identified that are separated by the static free shear flow boundary. The peak current was sensitive to cathode placement relative to this flow structure and could be scaled from ~300 mA to over 5 A. Applying a Boltzmann equation solver, it was found that ~1% air entrainment into the flow and an $E/N \lesssim 5\times10^{-16}$ V cm^{-2} could account for the observed trends.

15. SUBJECT TERMS
optical spectroscopy, Plasma Physics

16. SECURITY CLASSIFICATION OF:			17. LIMITATION OF ABSTRACT:	18. NUMBER OF PAGES	19a. NAME OF RESPONSIBLE PERSON (Monitor)
a. REPORT	b. ABSTRACT	c. THIS PAGE			Biswa N. Ganguly
Unclassified	Unclassified	Unclassified	SAR	10	19b. TELEPHONE NUMBER *(Include Area Code)* N/A

Standard Form 298 (Rev. 8-98)
Prescribed by ANSI Std. Z39-18

Current scaling in an atmospheric pressure capillary dielectric barrier discharge

Brian L. Sands,[1,a)] Shih K. Huang,[2] and Biswa N. Ganguly[3,b)]
[1]*UES, Inc., 4401 Dayton-Xenia Rd., Dayton, Ohio 45432, USA*
[2]*Department of Mechanical and Materials Engineering, Center for Advanced Power and Energy Conversion, Wright State University, 3640 Colonel Glenn Hwy., Dayton, Ohio 45435, USA*
[3]*Air Force Research Laboratory, 2645 5th St., Wright Patterson Air Force Base, Ohio 45433, USA*

(Received 4 June 2009; accepted 6 July 2009; published online 4 August 2009)

Current scaling in an atmospheric pressure capillary dielectric barrier discharge, comprising a structured rare gas flow that extends into ambient air, is characterized by electrical and optical measurements. In the transient glow mode, two current scaling regimes were identified that are separated by the static free shear flow boundary. The peak current was sensitive to cathode placement relative to this flow structure and could be scaled from ~300 mA to over 5 A. Applying a Boltzmann equation solver, it was found that ~1% air entrainment into the flow and an $E/N \lesssim 5\times10^{-16}$ V cm^{-2} could account for the observed trends. © *2009 American Institute of Physics*. [DOI: 10.1063/1.3187939]

Research into the generation of stable, nonequilibrium atmospheric pressure plasmas has been growing significantly in part because these plasma sources have the potential to impact a diverse variety of fields from materials engineering to biomedicine.[1] One type, the atmospheric pressure plasma jet, utilizes a gas flow, typically helium, which is energized to form a plasma that extends into ambient air. In the configuration studied here,[2–5] the plasma channel within the gas flow is formed by a rapidly propagating self-sustained ionization front, a streamerlike discharge, rather than existing as an afterglow plasma effluent from a remote source. With a grounded electrode downstream, a capillary dielectric barrier discharge (CDBD) can be established.[6] This configuration has been shown to have significant advantages in terms of enhanced plasma chemistry at atmospheric pressure,[7] and has recently been used to demonstrate the high-speed deposition of SiO_2 films.[8] This motivates a more detailed look at the properties of the discharge and the factors that can affect the plasma chemistry near the substrate. In this letter, we demonstrate the spatiotemporally resolved evolution of the streamer-to-glow transition for this CDBD. While this CDBD evolves much like a single microdischarge in a typical pulsed coplanar DBD, this source has unique properties owing to the structured gas flow through which the current channel is established. We will show that the placement of the cathode relative to this gas flow structure significantly alters the current scaling in the transient glow phase. Two regimes for current scaling are identified that are clearly separated by the static free shear flow boundary that exists between the rare gas core flow and the surrounding air.

The experimental configuration is shown in Fig. 1. An equivalent circuit diagram for the CDBD is displayed in the inset. A single 2 cm long nickel electrode was placed at 12 mm from the edge of a Pyrex capillary with an inner diameter of 2 mm and an outer diameter of 3 mm. This is represented in the circuit diagram as C_a. A 95% helium, 5% argon gas mixture, hereafter referred to as the He/Ar mixture, flowed through the capillary at a rate of 2.0 standard l/min, establishing a free shear flow beyond the confines of the capillary. A planar aluminum electrode was placed downstream at a variable distance d from the capillary tip, defining C_g. A Teflon dielectric film C_d, with thicknesses of 50.8 and 254 μm, was alternately used on the cathode to simulate a target substrate for material processing. This was grounded through a 1 kΩ load resistance R_L. To drive the CDBD, we used a 12 kV, positive unipolar voltage pulse, with a rise time of 10 ns, switched at a 1 kHz rate. These represent the nominal conditions for this experiment. The flow rate, mixture ratios, and driving parameters were kept constant.

Optical emission was monitored using two photomultiplier tubes (PMTs) having a rise time of 2 ns. The emission was fiber coupled from detectors focused on the capillary axis with a spatial resolution of ~1 mm and was corrected for inherent signal delays. A reference PMT detector was fixed 1 mm from the capillary tip while the other detector was fixed 1 mm from the movable cathode. To the detectors we affixed 10 nm bandpass filters to measure emission from Ar $2p_1 \rightarrow 1s_2$ at 750 nm, $N_2C\ ^3\Pi_u \rightarrow N_2B\ ^3\Pi_g$ at 337 nm,

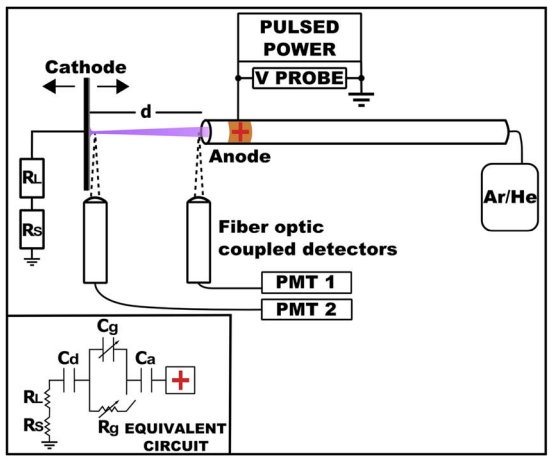

FIG. 1. (Color online) Schematic of the CDBD experimental apparatus and associated diagnostics. An equivalent circuit diagram of the CDBD portion of the circuit is shown in the inset.

a)Electronic mail: brian.sands@wpafb.af.mil.
b)Electronic mail: biswa.ganguly@wpafb.af.mil.

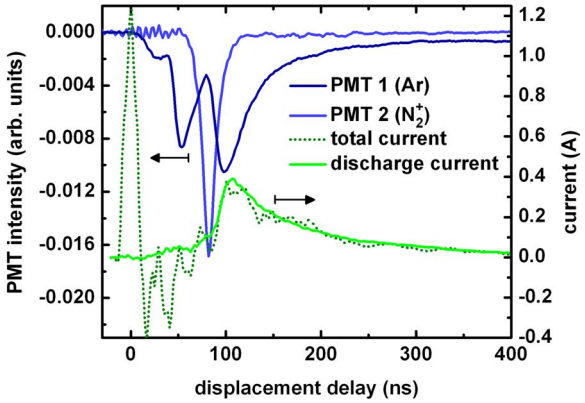

FIG. 2. (Color online) Temporally resolved current and PMT emission profiles showing the streamer-glow transition for the CDBD at a gap separation of 20 mm.

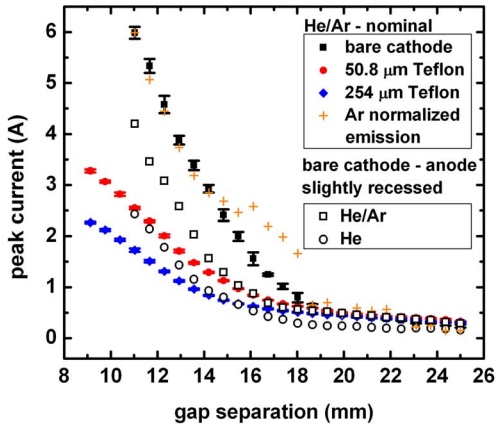

FIG. 3. (Color online) Current scaling in this CDBD configuration as a function of gap separation for a 95% He/5% Ar mixture and for a pure He case using the bare cathode. 750 nm PMT emission from Ar is also shown normalized to the nominal He/Ar bare cathode current.

and $N_2^+B\ ^2\Sigma_u \rightarrow N_2^+X\ ^2\Sigma_g$ at 391 nm. These emission features were among the brightest in the discharge spectrum. The electrical properties of the discharge were monitored with a wide bandwidth Tektronix P6015 voltage probe connected at the anode and a current sensing resistor R_s, with an effective resistance of 8.3 Ω, attached to the cathode. The PMT and probe signals were averaged over 1000 shots.

The characteristic evolution of this capillary dielectric barrier discharge is shown in Fig. 2, using a Teflon covered cathode, as this acted to further stabilize the discharge, allowing for a more precise view of the discharge process. The gap separation was 20 mm. The discharge current is superimposed onto the total current and the peak of the displacement current marks $t=0$. The PMTs were not calibrated for wavelength-dependent emission intensities so they cannot be quantitatively compared. PMT 1 depicts emission from excited Ar near the capillary tip while PMT 2 shows emission from N_2^+ near the cathode surface. The primary streamer can be tracked starting with the first large peak from PMT 1 as the streamer exits the capillary. The strong emission peak from N_2^+ marks the arrival of the streamer at the cathode. This emission is enhanced as the streamer approaches the cathode and the local E/N, where E is the electric field and N is the gas density, increases. The bridging of the gap by the streamer is correlated with a sharp rise in current as the discharge transitions to the transient glow mode. The discharge current peak coincides with a second peak in emission near the capillary tip that is associated with the slowly propagating "secondary streamer" that is characteristic of the low E/N transient glow mode.[9] This discharge process is also illustrated in a time-resolved broadband image sequence acquired with an intensified charge-coupled device camera under conditions close to those in Fig. 2 that is included as a media supplement to this letter.[10]

Figure 2 shows that the basic discharge process is very similar to other pulsed DBD configurations. However, as the gap separation is varied, Fig. 3 shows that the current scaling is not consistent with a simple variation of E/N in the transient glow mode. Data for the bare cathode and various cathode composites are shown using the He/Ar flow gas mixture under nominal conditions. The bare cathode was also tested in a pure He flow. For this case, the anode was slightly recessed so as to decrease C_a; measurements were then repeated for the He/Ar mixture for comparison. The error bars for the current measurements under nominal conditions represent the standard deviation of three successive runs to demonstrate the stability of the CDBD, which is noticeably better in the case of a dielectric covered cathode.

Starting with an initial gap separation of 25 mm, Fig. 3 shows the measured current increased slowly over the first 5 mm with little relative variation among the different cases except for a noticeable offset in the pure He case. When the cathode was drawn within 20 mm of the capillary tip, the measured current increased more rapidly depending on the cathode material, anode separation, and flow gas composition. For the bare cathode, the transition between these two regimes was more pronounced and was somewhat muted in the other cases. For example, in the case of the He/Ar mixture, the peak current nearly doubled over a space of 2 mm from ~450 mA at 20 mm. Figure 3 also shows that the increase in current is mostly tracked by a proportionate increase in emission from excited Ar, acquired from PMT 2, and normalized to the He/Ar bare cathode current. The measured Ar emission intensity tracked the current in the dielectric cases as well; however, emission from the air plasma species monitored in this experiment did not track the current indicating the importance of the rare gas core for current scaling.

The data in Fig. 3 show that there are two distinct regimes for current scaling in this CDBD source that are separated by a transition at a gap separation of ~20 mm under our flow conditions. This is a unique property of this particular DBD source that can be explained by the varying structure of the gas flow that comprises the discharge medium and its effect on the local plasma conductivity as the cathode position is varied. In the following discussion, we refer to the equivalent circuit shown in Fig. 1. We reduce the CDBD to a parallel gap capacitance C_g and lumped resistance R_g, both in series with a dielectric capacitance. The dielectric capacitance can be split into contributions from the capillary tip C_a and the cathode C_d if a dielectric film is present. The lumped resistance R_g depends inversely on the conductivity of the gas in the current channel. Under the assumption of glow discharge conditions after the streamer has bridged the gap, we used the Boltzmann equation solver BOLSIG+ (Ref. 11) to estimate the fundamental quantities that make up the conductivity, to help explain the data in Fig. 3. The conductivity σ in the time domain is given by,

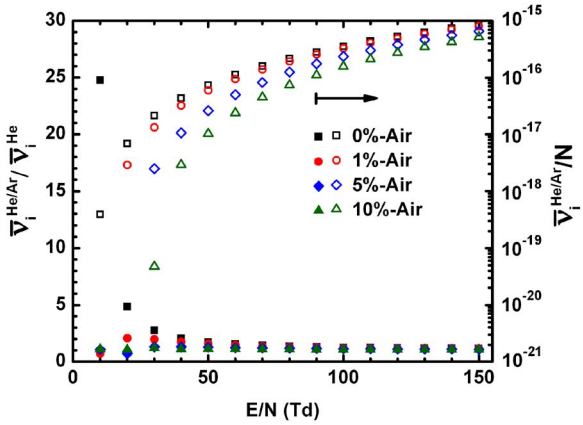

FIG. 4. (Color online) BOLSIG+ calculations showing the ratio of ionization frequencies of a 95% He/5% Ar mixture to the pure He case (left) and the ionization frequency in the He/Ar mixture (right) for several mole fractions of air.

$$\sigma(t) = e\mu_e n_0 \exp(\bar{\nu}_i t), \tag{1}$$

where $\bar{\nu}_i$ is an effective ionization frequency taking attachment into account. The electron mobility is denoted by μ_e. The electron charge and initial electron number density are denoted by e and n_0, respectively. The BOLSIG+ solver assumes a spatially uniform and steady state electric field. Consequently, since σ varies in time, we restrict our interpretation of model calculations to describing only the initial conditions in the transient glow mode. We assumed a composition of both pure He and 95% He/5% Ar with varying mole fractions of air ($79\%N_2/21\%O_2$) up to 10%, simulating the progressive entrainment of air into the rare gas core flow. Only direct electron impact ionization processes were considered for electron density growth. The E/N was varied between 10 and 150 Td. The important results are summarized in Fig. 4. The ratio of the He/Ar ionization frequency $\bar{\nu}_i^{\mathrm{He/Ar}}$ to the He ionization frequency $\bar{\nu}_i^{\mathrm{He}}$ is plotted versus E/N for different mole fractions of air on the left axis. The range of calculated $\bar{\nu}_i^{\mathrm{He/Ar}}/N$ is shown on the right axis. The missing values in Fig. 4 indicate where $\bar{\nu}_i^{\mathrm{He/Ar}}/N$ was calculated to be negative, indicating that attachment from the air impurity is dominating. The electron mobility was found not to vary as significantly as $\bar{\nu}_i$ and is not considered further.

When the cathode is in the rare gas core flow, for $d \lesssim 20$ mm, the measured current is significantly larger for the He/Ar mixture than for He alone (open symbol cases). For $d > 20$ mm, the measured current for all cases converge to a single trend that is largely independent of the flow mixture or cathode material. In Fig. 4, the ratio $\bar{\nu}_i^{\mathrm{He/Ar}}/\bar{\nu}_i^{\mathrm{He}}$ favors the He/Ar mixture with no air impurity, but this ratio decreases significantly with just 1% air entrainment for $E/N < 30$ Td and approaches unity for >1% air entrainment, independent of E/N. For $E/N > 50$ Td, the effect of air entrainment is comparatively small. This can explain the data in Fig. 3 as a transition from the rare gas core flow to a mixed gas regime characterized by air entrainment. The measured current for He/Ar in this mixed gas regime is still measureably greater than for the He case, but it is converging toward the He value. Figure 4 then suggests the amount of air entrainment at the transition to this regime is likely closer to 1% when $\bar{\nu}_i^{\mathrm{He/Ar}}/\bar{\nu}_i^{\mathrm{He}} > 1$. This agrees with experimental measurements taken with the "plasma needle" that place this value as low as 0.5%.[12] Additionally, for progressive air entrainment to account for the observed trends in Fig. 3, this implies that the E/N in the plasma channel in the transient glow mode is $\lesssim 50$ Td. Indeed, this is consistent with a rough estimate of the E/N simply from the ratio of applied voltage to gap separation. The dependence of the current scaling on the dielectric capacitance in the two regimes can also be explained from Fig. 4. Increasing the Teflon film thickness will decrease the gap E/N. From Fig. 4, $\bar{\nu}_i^{\mathrm{He/Ar}}/N$ is significantly reduced in the presence of air for $E/N < 30$ Td. However, Eq. (1), on the timescale of the current rise (order 10 ns), suggests that the local conductivity is insensitive to these changes in the mixed gas regime as the exponential growth term will approach unity at low E/N. Therefore, the current should follow E/N linearly in this regime, which is slowly varying assuming $E/N \propto 1/d$, independent of the dielectric capacitance. This is justified in Fig. 3 for $d > 20$ mm. Conversely, when the cathode is brought into the rare gas core flow (0% data), Fig. 4 shows that $\bar{\nu}_i^{\mathrm{He/Ar}}/N$ can increase abruptly in the absence of air at low E/N. The exponential dependence on $\bar{\nu}_i$ in Eq. (1) is now more significant and the sensitivity of $\bar{\nu}_i$ to E/N has a greater effect on the conductivity. For $E/N < 50$ Td, $\bar{\nu}_i^{\mathrm{He/Ar}}/N$ varies by almost three orders of magnitude. Again, since the gap E/N is lower with increasing dielectric thickness, the gap separation then needs to be smaller than in the bare cathode case to yield a significant increase in the conductivity. This can explain the dependence of current scaling on dielectric thickness for $d < 20$ mm in Fig. 3 as the marked increase in current occurs at smaller gap separations for increased dielectric thickness. The BOLSIG+ calculations show that with a small incorporation of air into the current channel, the channel conductivity is determined primarily by the air impurity. This can account for the observed current scaling trends.

We thank Jared Speltz and Matthew Niekamp for their assistance. This work was partially supported under U.S. Air Force Contract No. FA8650-04-D-2404.

[1] M. Laroussi and T. Akan, Plasma Processes Polym. **4**, 777 (2007).
[2] M. Teschke, J. Kedzierski, E. G. Finantu-Dinu, D. Korzec, and J. Engemann, IEEE Trans. Plasma Sci. **33**, 310 (2005).
[3] J. Shi, F. Zhong, J. Zhang, D. W. Liu, and M. G. Kong, Phys. Plasmas **15**, 013504 (2008).
[4] B. L. Sands, B. N. Ganguly, and K. Tachibana, Appl. Phys. Lett. **92**, 151503 (2008).
[5] K. Urabe, Y. Ito, K. Tachibana, and B. Ganguly, Appl. Phys. Express **1**, 066004 (2008).
[6] J. Walsh, J. Shi, and M. Kong, Appl. Phys. Lett. **88**, 171501 (2006).
[7] J. L. Walsh and M. G. Kong, Appl. Phys. Lett. **93**, 111501 (2008).
[8] Y. Ito, K. Urabe, N. Takano, and K. Tachibana, Appl. Phys. Express **1**, 067009 (2008).
[9] E. Marode, J. Appl. Phys. **46**, 2005 (1975).
[10] See EPAPS supplementary material at http://dx.doi.org/10.1063/1.3187939 for a time-resolved image sequence of the discharge process.
[11] G. J. M. Hagelaar and L. C. Pitchford, Plasma Sources Sci. Technol. **14**, 722 (2005).
[12] I. E. Kieft, J. J. B. N. van Berkel, E. R. Kieft, and E. Stoffels, Proceedings of the 16th International Symposium on Plasma Chemistry, 2005, Vol. 22, pp. 295–308.